ISSN 8755-6839

SCIENCE OF **TSUNAMI HAZARDS**

Journal of Tsunami Society International

Volume 37 **Number 4** **2018**

ANALYSIS OF TRAVEL TIME DELAY FOR LARGE TSUNAMIS ACROSS THE PACIFIC AND INDIAN OCEANS

Tjipto Prastowo[1,2], Latifatul Cholifah[2], Madlazim[1,2]

[1]Physics Department, State University of Surabaya, Surabaya 60231, Indonesia
[2]Center for Earth Science Studies, State University of Surabaya, Surabaya 60231, Indonesia
Correspondence: madlazim@unesa.ac.id

ABSTRACT

Travel time delay for a tsunami has been an increasingly important issue in recent years. The delay in time is calculated from a difference in arrival times between simulated waveforms and waves recorded by DART and gauge stations. In this study, we estimate travel times for the 2011 Tohoku, the 2014 Iquique, the 2004 Aceh, and the 2010 Mentawai events. We compare estimated travel times with travel times from field records and find that the time delay is increasing with epicentral distance, following reduced speeds during propagation. From analyses of the delays, we conclude that speed reduction in the Pacific is 1-2% from the long-wave speed but twice larger or more in the Indian Ocean due to its complex bathymetry. For far-field propagation in the Pacific, the delays could be approximately 17 minutes whereas the same amount of delay was attained at a shorter distance in the Indian Ocean.

Keywords: *travel time delay, estimated travel times, epicentral distance, speed reduction*

1. INTRODUCTION

Disaster early warning issues are of primary importance in the sense that the accurate and quick release of early warning may prevent society from potential losses of lives, properties, and infrastructures. The occurrence of a tsunami wave on a beach, for example, needs to be predicted accurately using rapid assessment of tsunami waveforms recorded by in-situ instruments and theoretical development of tsunami propagation modeling. In this regard, this current work examines arrival times of a tsunami wave detected by a regional network of seismic stations either positioned nearby or at far away from the source location. With respect to tsunami onset times, these quantities lead to observed travel times of tsunami wave propagation at an open sea. In the context of hazard mitigation study, particularly critical problems with disaster preparedness and risk reduction efforts for vulnerable countries in the Indian Ocean zone (Suppasri et al. 2015), knowledge of accurate travel times, both measured and predicted, is required for minimizing possible fatalities imposed by such a catastrophy (Cholifah and Prastowo, 2017).

Regarding the above backgrounds, research focusing upon the difference in travel times between observed waves and simulated waveforms has thus been an increasingly important issue in recent years. Since then, many researchers (e.g., Wessel, 2009; Inazu and Saito, 2013; Allgeyer and Cummins, 2014; Wang, 2015) have reported that trans-oceanic large tsunamis propagating across the ocean with a total travel distance of exceeding thousands kilometers away show a departure of observed travel times from predicted values based on the shallow-water, long-wave theory. This departure is called travel time delay in the present study, which is arguably attributed to variations in tsunami phase speed, as addressed in previous studies (Tsai et al. 2013; Watada, 2013; Watada et al. 2014; Gusman et al. 2015). All of these studies have used a combined method of exploring tsunami numerical modeling with some assumptions to take into account for the linear approximation and field data observations for comparison.

In the following sections, we provide basic physics principles for shallow-water, long-wave approximation usually made for use of numerical modeling of tsunami wave propagation at an open sea (Fine et al. 2013; Heidarzadeh et al. 2014). Seawater is assumed to be incompressible and homogeneous with no vertical stratification (see, for example, Wang, 2015) and hence vertical profile of seawater density is assumed to be constant with depth. There is no shear at both the sea surface and sea bottom, and hence effects of wind-induced forcing and other external influences are not included in the governing equations. In the absence of local circulation in the ocean by diffusion (Prastowo et al. 2017), the only driving force for the horizontal advection of massive mass and volume fluxes of seawater is seismic energy released from fault movement at depth. Vertical variation in the sea surface elevation is merely considered to be important during the passage of a gigantic tsunami wave that propagates over a long distance along a stationary, flat-bottomed seafloor. However, tsunami wave height or its corresponding wave amplitude is assumed to be relatively small compared with tsunami wavelength and water depth (Cholifah and Prastowo, 2017). Therefore, the small-amplitude wave theory during tsunami propagation remains useful. Non-linearity effects of higher-order terms imposed by the free sea surface and rigid bottom boundary conditions in the equations of motion are also negligible.

All of the above assumptions lead to the well-known linear, shallow-water, long-wave propagation of a tsunami wave, written as momentum equation below

$$\partial \mathbf{u}/\partial t = - g d \, (\partial/\partial x + \partial/\partial y)\eta \quad (1)$$

where **u** is the depth-integrated horizontal velocity of the wave with $\partial \mathbf{u}/\partial t$ represents the tsunami speed evolution with time, g is gravitational acceleration due to the Earth's gravity, d is the ocean depth, and η is the sea surface elevation. The corresponding continuity equation is as follows,

$$\partial\eta/\partial t + (\partial/\partial x + \partial/\partial y)\mathbf{u} = 0 \quad (2)$$

simply describing conservation of mass for incompressible fluid of seawater (see Prastowo and Ain, 2015). After some simple algebra, the theoretical speed c of a propagating tsunami can be obtained as follows,

$$c = (gd)^{1/2} \quad (3)$$

For a typical water depth of $d \sim 5$ km, the tsunami speed is about 720 km/h.

Inazu and Saito (2013) proposed a local parameter β taken into account from loading effects of seafloor deformation. This parameter introduces the roles of non-stationary sea bottom over bathymetry in the form of a reduced wave height $\eta - \eta_o$ measured from the sea surface into the momentum equation, where η_o is associated with the depth through which seabed is deformed. Equation (1) then becomes

$$\partial \mathbf{u}/\partial t = - g d \, (\partial/\partial x + \partial/\partial y)(\eta - \eta_o) \quad (4)$$

with equation (2) remains true but with an additional equation relating η to η_o via the β parameter, that is, $\eta = \beta\eta_o$ over which tsunami speed reduction due to the Earth elasticity is in effect. Wang (2015) further explained that β was found to be relatively small to account for the depth-corrected speed of only 1% from the theoretical long-wave speed. This parameter limits the observed speed to only a small amount of tsunami speed reduction for near-field and far-field (Inazu and Saito, 2013; Wang, 2015) according to

$$c = (gd)^{1/2}\ (1-\beta)^{1/2} \tag{5}$$

Noting that equation (5) is particularly applicable to distant observations, we here argue that the speed is reduced while propagating over large distances across the ocean with complex bathymetry, as suggested by Tsai et al. (2013) and Watada (2013). This speed reduction is observed as the apparent difference in tsunami travel time between numerical simulations (*e.g*., Allgeyer and Cummins, 2014; Watada et al. 2014; Gusman et al. 2015) and field observations by monitoring Deep-ocean Assessment Reports of Tsunamis (DART) buoys and tide-gauge instruments.

In this study, we extract estimates of tsunami travel times from tsunami waveforms of four large tsunami events that occurred in the Pacific and Indian Oceans and then compare estimated travel times with observed travel times from field records obtained from wide-spread network of coastal and mainland observatories using either DARTs or tide gauges. We carefully examine and analysis the delay in time derived for each case considered in relation to increasing travel distance. Therefore, the primary aims of the present study are to see if there is a systematic increase in the delays with epicentral distance for all trans-oceanic tsunamis examined in this study and to determine whether the increase is associated with speed reduction, as predicted by equation (5).

2. METHOD

The methods used in this study included procedures for research design, as shown in Figure 1, numerical data collection from observed waves and simulated waveforms, and data analysis technique.

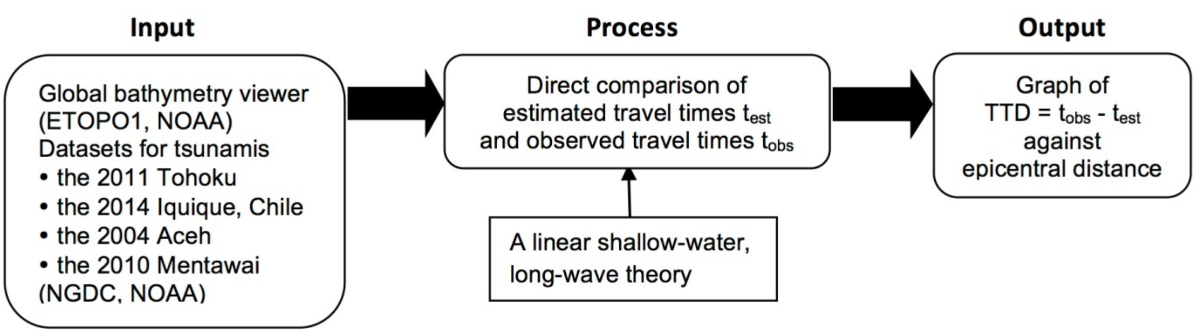

Figure 1. Simple diagram, showing steps at obtaining travel time delay (TTD) against epicentral distance.

We examined four cases of trans-oceanic large tsunamis: two events in the Pacific Ocean, namely the Tohoku tsunami with M_w 9.0 and the epicenter was located at 38.3^o N and 142.4^o E, occurred on

March 11, 2011 at 05:51 UTC off the east-coast of the Tohoku district, Japan and the Chile event with M_w 8.2 and the epicenter was positioned at 19.6° S and 70.8° W, occurred on April 1, 2014 at 23:47 UTC off the coast of Iquique, Chile, and other two occurrences in the Indian Ocean, namely the Aceh tsunami with M_w 9.1 and the epicenter at 3.4° N and 95.7° E, occurred on December 26, 2004 at 01:18 UTC off the west-coast of Meulaboh, Aceh, and the 2010 Mentawai tsunami with a lesser magnitude of M_w 7.7 and the epicenter at 3.5° S and 100.1° E, occurred on October 25, 2010 at 14:42 UTC off the west-coast of Mentawai island (here UTC is used for the abbreviation of Universal Time Coordinate).

For each case tsunami considered, we provided a number of numerical datasets of travel times collected from direct comparison of simulated waveforms (see Rabinovich et al. 2011; Inazu and Saito, 2013; Satake et al. 2013; Watada et al. 2014; Gusman et al. 2015) and those recorded by the monitoring DARTs and gauges managed by the National Oceanic and Atmospheric Administration (NOAA) at various geographical locations around the globe. The locations of the buoys and the gauges with the resulting observed tsunami travel times were accessed at https://www.ngdc.noaa.gov. The global bathymetry viewer was accessed at https://maps.ngdc.noaa.gov/viewers/bathymetry/ and the corresponding data was accessed at https://ngdc.noaa.gov/mgg/global/relief/ETOPO1/ for careful examinations of the complex bathymetry of the two Oceans. From the two corresponding values of travel times, both measured and predicted values, we derived paired datasets in the present study and the paired datasets allowed us to simply calculate travel time delay. The delays were then tabulated and here classified into three observational regions (see Cholifah and Prastowo, 2017), depending upon a DART or gauge location measured from the source, namely near-field, intermediate-field, and far-field zonal tsunami observations. Watada et al. (2014) and Gusman et al. (2015) argued that zones of measurements were only near-field and far-field observations but these different views gave no different qualitative results.

Following Cholifah and Prastowo (2017), we argued that near-field data were records provided by the DARTs and the gauges of less than 3,000 km away from the epicenter. Data for intermediate-field were directly obtained from the two types of instruments positioned in the ranges 3,000-12,000 km. Far-field data observations were given by monitoring stations located at a distance of more than 12,000 km away. In comparison with estimated travel times, these measured travel times led to the apparent time delay. For all cases considered in the present study, we analyzed the data for the delays, which were plotted against epicentral distance to see the nature of the delay in correspond to increasing travel distance for each case. We then analyzed different pathways and mechanisms of tsunami wave propagation between the Pacific and the Indian Ocean tsunamis and thus determined possible sources of increasing time delay in relation to tsunami speed reduction induced by geophysical disturbances during tsunami propagation. The results for all events are discussed in terms of the speed reduction, as predicted in equation (5) by Inazu and Saito (2013), as well as tsunami energy dissipation while propagating away from the source.

RESULTS AND DISCUSSION

The results for all the Pacific and Indian Ocean tsunamis considered in the present study are given in the forms of tables and corresponding graphs. Regarding apparently different characteristics of the two Oceans, we provide the 2011 Tohoku and the 2014 Chile events as the first two cases discussed then followed by the 2004 Aceh and the 2010 Mentawai tsunamis as the last two major events to discuss. Corresponding graphs for each case are generated by time delays resulted from the paired datasets of observed and predicted tsunami travel times and by epicentral distances at which the delays to occur for all observational points of view contributed from field measurements by the buoys and the gauges.

Table 1 provides a coded list of 13 DART buoys distributed over different geographical locations used in the present study, covering all zones of tsunami observations from near-field to far-field regions and resulting travel times from numerical simulations and direct observations. The apparent difference in travel time is again defined as travel time delay, which is here measured in minutes in the last column.

Table 1. The paired datasets for the 2011 Tohoku tsunami occurrence with travel time delay is calculated from the difference between observed and estimated travel times for each DART code.

DART Code	Observational Location	Latitude	Longitude	Epicentral Distance (km)	Estimated Travel Time (h)	Observed Travel Time (h)	Travel Time Delay (min)
21413	near-field	30.51° N	152.12° E	1,246	1.29	1.30	0.6
21415	near-field	50.18° N	171.85° E	2,670	3.14	3.18	2.4
52402	intermediate	11.88° N	154.12° E	3,165	3.71	3.76	3.0
52403	intermediate	4.05° N	145.59° E	3,828	4.91	4.97	3.6
46409	intermediate	55.30° N	211.48° E	5,344	6.71	6.78	4.2
52406	intermediate	5.29° S	165.00° E	5,388	6.71	6.80	5.4
51407	intermediate	19.59° N	203.41° E	6,183	7.63	7.74	6.6
51425	intermediate	9.51° S	183.76° E	6,839	8.11	8.23	7.2
46411	intermediate	39.35° N	232.98° E	7,486	9.23	9.35	7.2
43412	intermediate	16.07° N	253.00° E	10,619	13.40	13.59	11.4
51406	intermediate	8.48° S	234.97° E	10,828	13.37	13.59	13.2
32411	far-field	4.99° N	269.16° E	12,741	16.57	16.82	15.0
32412	far-field	17.97° S	273.61° E	14,816	18.90	19.18	16.8

The paired datasets listed for time delays indicate that all observed tsunami waves in nature arrive later relative to simulated tsunami waveforms from a couple of minutes to teens of minutes for further stations. In other words, the delays in time increase with increasing epicentral distance measured from the source. This suggests that tsunami speed slows down at places far away from the epicenter. This is sensible in that at remote regions the speed predicted by equation (5) is slowed down by ~ 1% from its theoretical value given by equation (3) for the long-wave approximation. The reduction in speed is attributable to effects of variable bottom topography at seabed induced by the elasiticity of the solid Earth, as claimed by some previous work (Inazu and Saito 2013; Allgeyer and Cummins, 2014; Watada et al. 2014; Gusman et al. 2015; Wang 2015; Cholifah and Prastowo, 2017). In order to make the speed reduction clear, we here provide a plot of the time delay on increasing epicentral distance for the Tohoku case in Figure 2.

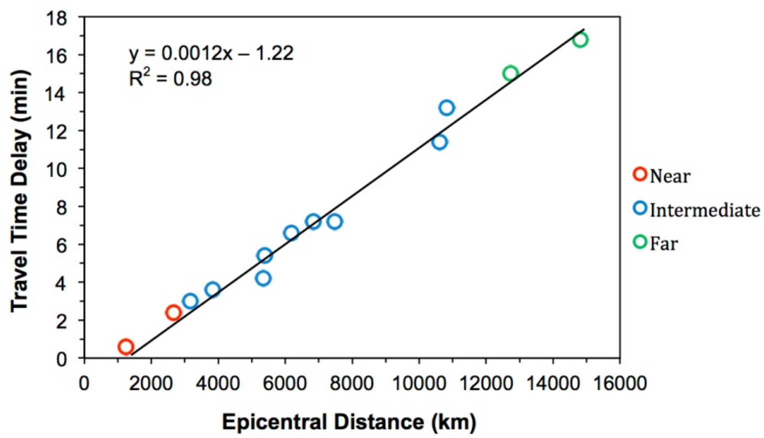

Figure 2. Travel time delay as a function of epicentral distance for the 2011 Tohoku event.

Some interesting points are made from the plot, where time delay is shown to be a linear function of epicentral distance. For total travel distances of less than 1,000 km away from the source (near-field regime) the delay is ignored, implying no apparent differences in travel times between observations and simulations. For this ignored delay, we argue that this covered travel distance is not much influenced by loading effects of the elastic Earth and thereby giving no delays in time. However, the near-field regime covers a travel distance of approximately 3,000 km away, taking a travel time of corresponding 4 hours for the Tohoku tsunami with a typical speed of 720 km/h to travel across the Pacific with small amounts of energy loss by dissipation during propagation and with no significant change in the waveforms due to insignificant geophysical disturbances (Watada, 2013; Allgeyer and Cummins, 2014; Watada et al. 2014). We found that the small speed reduction in the near-field regime (red open-circles) is associated with a small amount of the delay, which is up to 1% of the estimated travel time of the linear long-wave.

For intermediate regime shown as blue open-circles in Figure 2, in the ranges 3,000-12,000 km, the delays appear to linearly increase with travel distance, confirming that the simulated waveforms with shorter travel times are leading to the observed waves. The delays in time are found between 3.0

and 15.0 minutes, which is consistent with previous work (Allgeyer and Cummins, 2014; Watada et al. 2014). As the distance increases, effects of geopotential disturbances as predicted by equation (5) is larger on the tsunami wave, resulting in a slightly larger reduction in speed, relatively compared with equation (3). The speed reduction varies from 1.3 to 1.6%, comparable with the 1% reported tsunami speed reduction in the same region of observation (Inazu and Saito 2013; Tsai et al. 2013; Wang, 2015).

For far-field observations where the wave travels to a travel distance of more than 12,000 km or equivalent to a travel time of more than 16 hours, a further speed reduction takes place, corresponding to a longer time delay of more than 15.0 minutes, shown as two green open-circles in Figure 2. However, the longer time delays in this regime give no significant change in the proportion of the speed reduction, relative to the long-wave speed. In other words, for remote areas a value of approximately 17 minutes only corresponds to a small reduction in tsunami speed valued for about 1.5% that is comparable with that for the intermediate observations (Inazu and Saito, 2013; Tsai et al. 2013; Allgeyer and Cummins, 2014; Watada et al. 2014; Gusman et al. 2015; Cholifah and Prastowo, 2017).

As stated in the previous paragraphs, the time delays are arguably owing to the speed reduction. This reduction is associated with energy dissipation when the wave encounters geophysical perturbations during its propagation across the Pacific. It follows that the reduction in speed may relate to pathways and mechanisms of tsunami energy decay in space and time as the wave advances away from the source. We discuss this issue in details later after all events are presented for comparison.

As comparison, Table 2 below provides a total of 19 DARTs at different geographical locations, marking observational regions from near-field to far-field zones. As also with Table 1, the datasets give travel times from simulations and observations. Again, the time delay is given in minutes.

Table 2. The paired datasets for the 2014 Chilean tsunami occurrence with travel time delay is calculated from the difference between observed and estimated travel times for each DART code.

DART Code	Observational Location	Latitude	Longitude	Epicentral Distance (km)	Estimated Travel Time (h)	Observed Travel Time (h)	Travel Time Delay (min)
32401	near-field	20.47° S	73.42° W	288	0.41	0.43	0.9
32402	near-field	26.74° S	73.98° W	853	1.15	1.18	1.7
32412	near-field	17.97° S	273.61° E	1,642	2.24	2.28	2.6
32413	near-field	7.40° S	266.50° E	2,797	3.79	3.85	3.5
32411	intermediate	4.99° N	269.16° E	3,505	5.38	5.43	2.6
43412	intermediate	16.07° N	253.00° E	5,595	8.24	8.29	3.5
46412	intermediate	32.46° N	239.44° E	7,838	11.65	11.74	5.6

DART Code	Observational Location	Latitude	Longitude	Epicentral Distance (km)	Estimated Travel Time (h)	Observed Travel Time (h)	Travel Time Delay (min)
46411	intermediate	39.35° N	232.98° E	8,770	12.88	13.00	7.1
51426	intermediate	22.99° S	191.87° E	9,869	13.68	13.78	6.5
51407	intermediate	19.59° N	203.41° E	10,301	13.96	14.09	8.0
46409	intermediate	55.30° N	211.49° E	11,036	16.18	16.35	10.6
46402	intermediate	51.07° N	195.98° E	11,904	16.59	16.76	10.6
21414	far-field	48.97° N	178.22° E	13,147	17.76	17.96	11.5
52406	far-field	5.29° S	165.00° E	13,304	18.53	18.71	10.6
21419	far-field	44.46° N	155.74° E	14,916	19.65	19.88	14.1
52401	far-field	19.26° N	155.77° E	15,134	20.35	20.55	11.8
52402	far-field	11.88° N	154.12° E	15,143	20.21	20.42	12.7
21418	far-field	38.71° N	148.69° E	15,660	20.42	20.67	14.9
52405	far-field	12.88° N	132.33° E	17,443	23.63	23.91	16.6

In general, the content of Table 2 is similar to that of Table 1. It follows that the behavior of tsunami propagation in the Pacific is independent of the propagation direction, whether the wave travels from the west Pacific to the east as in the Tohoku or on the other way around as in the Iquique tsunami. From the datasets provided in Table 2, we can examine that all time delays are due to the late arrivals of the observed waves detected at all nearby and far stations. The delays for the 2014 Iquique tsunami are in the ranges 10.6-16.6 minutes for far-field, comparable with 15 minutes of delay for the same regime of observation (Heidarzadeh et al. 2014). This trend in minutes of delay tends to be similar to that for the Tohoku case, implying that the speed reduction is similar for the Tohoku and Iquique tsunamis during tsunami propagation across the Pacific. Whereas Gusman et al. (2015) addressed the delays for distant propagation recorded by far-field stations at a longer travel time by 1-2% compared with predicted travel time, we claim the same amount of proportion for the speed reduction (see, for the 2011 Tohoku event, Cholifah and Prastowo, 2017). All delayed signals observed by DARTs for the Pacific tsunamis were found to correspond to β given in equation (5), introduced as variations in bottom topography (Inazu and Saito, 2013). For direct comparison, we here plot the time delay against epicentral distance for the 2014 Iquique event in Figure 3 below.

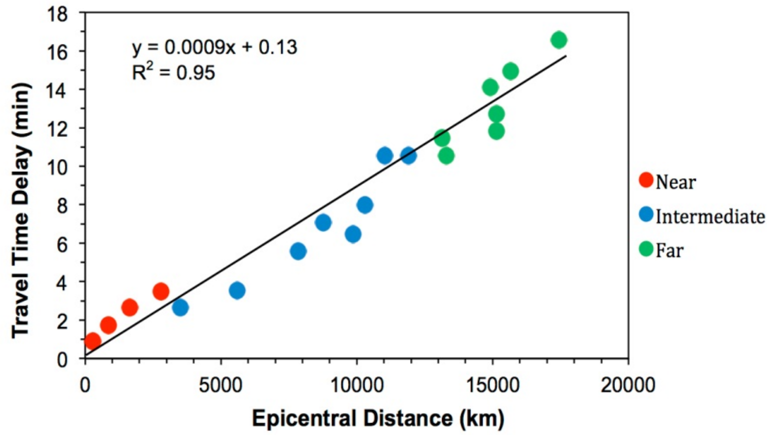

Figure 3. Travel time delay as a function of epicentral distance for the 2014 Chilean event.

Again we have time delay to be a linear function of travel distance for the 2014 Chilean event. For travel distances of less than 1,000 km in the near-field zone the delay remained less than 2 minutes, considered unimportant for tsunami early warnings. This ignored influence of the Earth elasticity effects upon the speed reduction goes further to only a short travel distance of about 1,500 km away, where topographical effects started to reduce the speed. With almost the same speed as in the case of the 2011 Tohoku tsunami, the loss in energy during propagation of the 2014 Iquique event in this field is only responsible for a small amount of the time delay (Gusman et al. 2015), accounted for about 1.5% of the estimated travel time calculated using the long-wave speed. For the intermediate and far regimes of observations, the time delays appear to linearly increase with increasing travel distance, again confirming similar behaviors of tsunami propagation in the Pacific. The maximum delay in the present study is up to 16.6 minutes achieved at a region of radius 17,500 km away from the source, close to the 15 minute-late arrivals of the observed waves reported by Heidarzadeh et al. (2014) for the Iquique event. This finding is also consistent with the maximum delay of 16.8 minutes for roughly the same distance in the 2011 event although the reasons for the delays reported by Cholifah and Prastowo (2017) did not include factors, such as seawater compressibility and geopotential variation, which may also be important for variations in tsunami speed in remote propagation. The point to make here is that a 1-2% speed reduction is found in the Pacific tsunamis, consistent with previous studies (Inazu and Saito, 2013; Tsai et al. 2013; Allgeyer and Cummins, 2014; Watada et al. 2014; Gusman et al. 2015).

For a complete examination, we provide in Table 3 below a number of tide-gauge stations at different locations in the Indian Ocean territory, listing observed and estimated travel times and hence time delay for each monitoring instruments used. Due to its complexity induced by complex bathymetry and different routes of tsunami propagation direction across the Indian Ocean (Rabinovich et al. 2011), we here only provide 5 paired datasets from tide-gauge field measurements, covering to only near-field and intermediate regimes of observations.

Table 3. The paired datasets for the 2004 Aceh tsunami occurrence with travel time delay is calculated from the difference between observed and estimated travel times for each tide-gauge station.

Tide Gauge	Observational Location	Latitude	Longitude	Epicentral Distance (km)	Estimated Travel Time (h)	Observed Travel Time (h)	Travel Time Delay (min)
Chennai	near-field	13.04° N	80.17° E	2,011	2.57	2.60	2.0
Male	near-field	4.18° N	73.52° E	2,441	3.25	3.42	10.0
Garcia	near-field	7.28° S	72.40° E	2,819	3.77	3.92	9.0
La Rue	intermediate	4.57° S	55.53° E	4,505	7.28	7.42	8.0
Lamu	intermediate	2.27° S	40.90° E	6,060	8.88	9.15	16.0

The results for the Indian Ocean tsunami show somewhat but clear difference in trend between increasing travel distance and its corresponding delays (see for example, gauge stations at Male, Garcia, and La Rue). These three stations measured a step decrease in the delay as travel distance increases, raising a question of whether the delay is a linear function of epicentral distance remains applicable for this case. However, the overall assessment derived from examination of signals arrived at Chennai, India, then one of the three stations at Male (Maldive islands), Diego Garcia, and Pointe La Rue in the open Indian Ocean up to Lamu observatory in the northern of Zanzibar (at the far east coast of Africa mainland) indicates a linearly positive correlation between time delay and epicentral distance for the 2004 event. What makes remarkably interesting here is that a maximum of 16.0 minute delay in this case was found for a much shorter travel distance, only at about 6,000 km away (the waves in the 2011 and 2014 events achieved approximately the same amount of such a time delay for more than doubled travel distance). Considering different properties of the Pacific and Indian Oceans, we speculate that this is an indicative of different tsunami pathways and mechanisms of propagation between the trans-Pacific tsunamis (the 2011 Tohoku and the 2014 Iquique occurrences) on one hand and the Indian Ocean tsunamis (the 2004 Aceh and the 2010 Mentawai events) on the other hand. To analyze further the distinguished characteristics between the two trans-oceanic tsunamis, we plot in Figure 4 (although with only limited points) time delay against travel distance for the 2004 Aceh event.

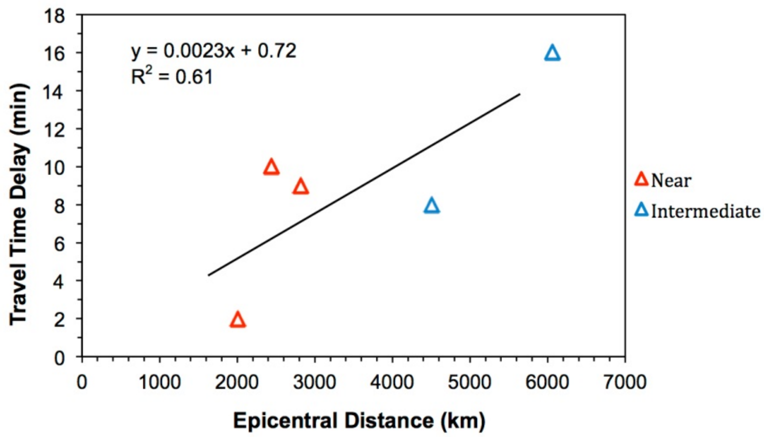

Figure 4. Travel time delay as a function of epicentral distance for the 2004 Aceh event.

Careful analysis of the determination coefficient represented by R^2 values and the slopes of lines of regression for each event from Figures 2, 3, and 4 reveal good arguments for the discrepancy in trend of time delay particularly for the Pacific and Indian Ocean tsunamis. In the case of the Pacific events, R^2 is found to be 0.98 for the 2011 Tohoku and 0.95 for the 2014 Iquique, providing a clear clue that dynamics of tsunamis in the Pacific is similar, independent of propagation direction and other regional perturbations owing to similar propagation characteristics. Thus, for a relatively large value of $R^2 \approx 1$ in the Pacific case, the delay is a remarkable linear function of travel distance measured from the source. The similar linear dependence of travel time delay on epicentral distance for the trans-Pacific tsunamis also indicates that the waves propagate along the same semi-enclosed ocean basin with the same level of roughness of bathymetry and that during the same amount of travel time they distribute the energy over long distances and dissipate it in the same fundamental mechanism of sea bottom friction along tsunami flow advection. Another interesting feature from Figures 2 and 3 to discuss is that the slopes in two regression lines are comparable, where they are rounded to 0.001 to three decimal places (within the considered unimportant errors of 0.0002 in all points from the near-field to the far-field for the 2011 Tohoku and the 2014 Iquique).

In contrast to the Pacific events, the data for the 2004 Aceh tsunami in the Indian Ocean show more scattered datapoints with a much smaller value of $R^2 = 0.61$ but this is in fact in good agreement with $R^2 = 0.59$ taken from "the west route" recorded by a network of coastal and mainland observatories discussed in the work of Rabinovich et al. (2011). Considering this primary finding in relation to Figure 4, we can say, to some extent, that the time delay is longer for a further travel distance but there is unlikely linear relationship between the delay and the epicentral distance for this case. We also find that the slope of the regression line for the 2004 Aceh tsunami is 0.002 (rounded to three decimal places), implying that the 2004 tsunami reached the same amount of time delay as the other two events in the Pacific Ocean but within a shorter distance, almost a half of that taken by the trans-Pacific tsunamis. The possible cause for this remarkable delay difference is that the Indian

Ocean is poorly understood with the more complex bathymetry and coarse topography along the direction line of tsunami propagation relatively compared with the Pacific Ocean, as implied by the works of Rabinovich et al. (2011, 2013). Another possible cause for the clear difference in the delays between the Pacific and the Indian Ocean tsunamis seems due to different mechanisms of energy decay. While advection dominates over diffusion in the Pacific in which the energy is dissipated in a rate that is much slower than that in the Indian Ocean, as also implied by Prastowo et al. (2017), the two mechanisms are in balance for the 2004 Aceh tsunami such that the loss of energy is controlled by both advection and diffusion effects.

Within the framework of a hypothetical strong influence of diffusion upon the speed reduction in the Indian Ocean tsunami, we here provide one more case study of another tsunami event that occurred in this region for a further clarification whether diffusion effects play a role in dissipating the energy and hence reducing the speed. Below is Table 4, consisting of datasets for the 2010 Mentawai case, where the data were obtained from field surveys (see Satake et al. 2013).

Table 4. The paired datasets for the 2010 Mentawai tsunami occurrence with travel time delay is calculated from the difference between observed and estimated travel times for each tide-gauge station.

Tide Gauge	Observational Location	Latitude	Longitude	Epicentral Distance (km)	Estimated Travel Time (min)	Observed Travel Time (min)	Travel Time Delay (min)
Padang	near-field	0.95° S	100.36° E	280	66.66	68.33	1.7
Tlk. Dalam	near-field	0.33° N	97.49° E	509	61.66	63.33	1.7
Cocos	near-field	12.11° S	96.89° E	1,013	81.66	81.86	0.2
Colombo	near-field	6.57° N	79.50° E	2,522	242.22	245.55	3.3
D. Garcia	intermediate	7.28° S	72.40° E	3,077	245.71	247.14	1.4
Rodrigues	intermediate	19.68° S	63.42° E	4,412	356.25	360.00	3.8
La Rue	intermediate	4.66° S	55.53° E	4,906	472.77	476.66	3.9
Port Louis	intermediate	20.15° S	57.50° E	5,033	432.50	442.50	10.0

The results for the 2010 Mentawai event in the Indian Ocean seem to have a similar behavior to those for the 2004 Aceh tsunami. The similarity of the two events can be concluded from the scatter of the data presented in Table 4. A relatively small amount of delay in time of only 0.2 minutes recorded by the Cocos-island observatory is likely due to its geographical location with respect to the source, where the island is directly positioned along the main path of tsunami energy distribution. As is the case for other events, travel time delay increases with travel distance for the 2010 Mentawai event (see, for example, Cholifah and Prastowo, 2017) owing to the Earth elastic loading in particular for distant propagation (see, for example, Inazu and Saito, 2013; Watada et al. 2014). However, there remains a question about the nature of the time delay in the sense that whether the delay is a linear function of increasing epicentral distance. To clarify this issue, we plot in Figure 5 time delay against travel distance for the 2010 Mentawai event.

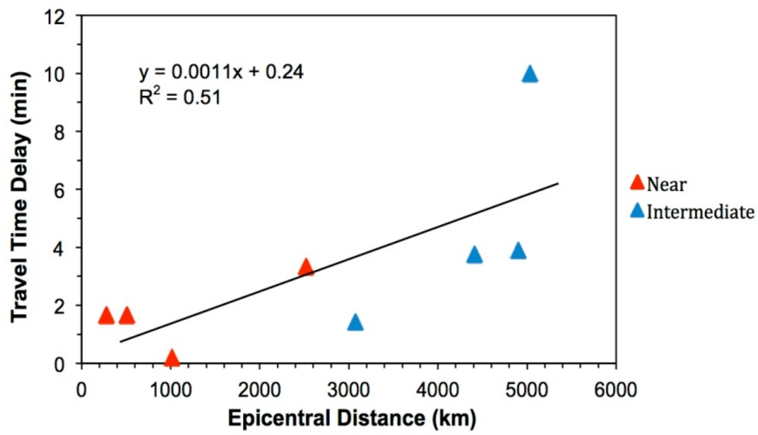

Figure 5. Travel time delay as a function of epicentral distance for the 2010 Mentawai event.

There is an interesting point to discuss from Figure 5. Noticeably, a value of $R^2 = 0.51$ was found for the 2010 Mentawai tsunami, comparable with that for the 2004 Aceh event (see Figure 4), indicating a similar behavior of tsunami propagation for both events. This is sensible because the two events were to occur in nearby regions off the west-coast of Sumatra with almost the same route for tsunami propagation across the Indian Ocean (see e.g., Rabinovich et al. 2011). Because a R^2 value is a statistical measure of the linearity of a given regression line, the relatively small values of R^2 for the Aceh and the Mentawai tsunamis confirm that the time delays in both events are not a linear function of increasing travel distance. It follows that relatively compared with the trans-Pacific tsunamis, the propagation of tsunami waves with the epicenters in the Indian Ocean is much affected by complicated sea bottom topography. As discussed by Prastowo et al. (2017) using a speed parameter of c/c_s where c is the theoretical long-wave speed and c_s is the complex speed (consisting of advection and diffusion components) applied to the 2010 Mentawai event, they showed that diffusion cannot be ignored in particular regions of the Indian Ocean. In this way, the rate of tsunami energy dissipation by horizontal flow advection and ocean diffusion for tsunami waves across the Indian Ocean is relatively higher than that for the trans-Pacific tsunamis. This argument is supported by the data in Tables 1 and 2 for the Pacific events compared with those in Tables 3 and 4 for the Indian Ocean tsunamis, where the same amount of time delay of ranging from 10 to 17 minutes is attained in a much shorter travel distance for tsunami waves that traveled in the Indian Ocean than those propagated in the Pacific.

Using a huge number of data for travel times from the Pacific and Indian Oceans, Wessel (2009) reported a significant departure of recorded travel times from predicted values of the linear long-wave theory. Although topographic disturbances were suspected as the possible cause for the late arrivals of the observed waves, he did not say about the speed reduction as the candidate for the corresponding travel time delay. There came about in several years later (see Tsai et al. 2013; Watada, 2013), where most of scientists started to realize that tsunami phase speed varies with both the internal factors, such as that given by seawater density variability and the external factors, such as that given by the dynamics of the elastic Earth in the form of seafloor deformation. In a careful examination using tsunami model of propagation for trans-Pacific tsunamis under influenced by effects of elastic loading, Watada et al. (2014) concluded that the observed speed could be reduced to 98% of the predicted the linear long-wave speed. It follows that the reduction in speed for the trans-Pacific tsunamis under consideration is of up to 2%. This magnitude of reduction is comparable with our findings of up to 3% reduction (including the 2004 Aceh and the 2010 Mentawai events) estimated from travel time delay in each case study (see Tables 1 and 2 for the Pacific events and Tables 3 and 4 for the Indian Ocean tsunamis). Using the field data for the Pacific occurrences as a reference for its linearity of time delays with respect to epicentral distances, we find that a 1-2% reduction in speed corresponds to $\beta = 0.02\text{-}0.04$ in this study, in good agreement with $\beta = 0.015\text{-}0.020$ reported by Inazu and Saito (2013) and further clarified by computational studies using additional effects of seawater compressibility and density variation in the ocean stratification (Allgeyer and Cummins, 2014; Watada et al. 2014; Gusman et al. 2015; Wang, 2015).

Other factors that may affect tsunami wave propagation in the open ocean include wave behavior, such as wave dispersion. Using the so-called "dispersion time" as the only single parameter examined in their computational work (Glimsdal et al. 2013), they claimed that the frequency-dependent speed is proved to be important for dispersive tsunamis especially in remote regions away from the source. This parameter is used to measure the effect of dispersion during tsunami propagation. For tsunamis of seismic origin with moderate magnitudes, the dispersion time was found relatively larger. It follows that these earthquakes may generate tsunami waves with frequency-dependent speed for all regimes of observations. However, for large tsunamigenic earthquakes this effect plays a role in reducing the speed for only at distant observations (Glimsdal et al. 2013). Although they did not relate their results to travel time delay, the consequence of the relative importance of dispersion effects on tsunami speed is clear in that the difference in tsunami speed between observations and simulations exists for particularly distant propagation. At this point, we could say that our findings in the case of the trans-Pacific tsunamis where a systematic linear increase in travel time delay against increasing travel distance are consistent with the work of Glimsdal et al. (2013). As travel distance increases, we speculate that the wave energy decays in time via dissipation due to advection, diffusion, and dispersion but this paper does not discuss these effects. Instead, this study focuses on analyzing travel time delay in relation to speed reduction.

The results for all regions of space for field monitoring of the Pacific and Indian Ocean tsunamis considered in the current study show surprising findings in the sense that while the time delay taken up by the computed and observed waves increases linearly for the case of the Pacific events, the proportion of the reduced speed is fixed with the speed reduction is valued between 1.0-1.6%, in good agreement with previous studies (Inazu and Saito, 2013; Tsai et al. 2013; Allgeyer and Cummins, 2014; Watada et al. 2014; Gusman et al. 2015; Cholifah and Prastowo, 2017). We believe that to some extent the qualitative results are independent of either the precise observations by the field monitoring instruments or the accuracy in predicted travel times by the numerical simulations. An improved numerical model of tsunami propagation by incorporating additional effects, such as compressibility of seawater upon the vertical stratification of the density field into the equations of motion, as suggested by Watada (2013), is therefore necessary for a better correction of the delays. It should be noted that there are at least two logical consequences that can be drawn from these findings. Firstly, it is true to conclude that tsunami speed varies primarily with the external parameters, such as effects of the complex bathymetry and the local topography induced by the elasticity of the solid Earth in the form of seafloor deformation on the non-rigid bottom topography (Allgeyer and Cummins, 2014; Watada et al. 2014; Gusman et al. 2015). Secondly, the speed reduction indicates that tsunami energy is lost due to dissipation by both advective flow of a tsunami wave and oceanic diffusion. The loss of energy, specified as energy decay in space and time during propagation in the Indian Ocean as discussed by Rabinovich et al. (2011) and in the Pacific as further investigated by Rabinovich et al. (2013), needs clarifying regarding estimates of energy dissipation in compressible fluids that go beyond of this study and therefore this issue, along with the inclusion of seawater compressibility in the equations of motion, is promising for future work.

3. CONCLUSIONS

Travel time delay for trans-oceanic tsunamis across the Pacific and Indian Oceans has been analyzed using paired datasets from simulated waveforms and field records from the DARTs and gauges. In this study, travel time estimates for the 2011 Tohoku, the 2014 Chilean, the 2004 Aceh, and the 2010 Mentawai events were compared with travel times from field records. Particularly for the Pacific tsunamis, the time delay is found to linearly increase with epicentral distance, suggesting that the speed is reduced during propagation. From careful analyses of the time delays, we conclude that the reduction in speed in the Pacific Ocean is 1-2% from the long-wave speed but it is twice or larger in the Indian Ocean owing to its complexity. For far-field propagation of more than 15,000 km in the Pacific, the time delays could be of up to 17 minutes while the same amount of travel time delay was achieved at a much shorter distance in the Indian Ocean.

Regarding the results for the Indian Ocean, where most coastal regions in the Sunda-arc islands within the Indonesian territories are vulnerable to geophysical hazards, including destructive tsunamis a number of more sensitive monitoring instruments are needed to detect the generation and propagation of a tsunami wave in the Ocean, and its arrival nearby and at shorelines. Therefore, near-field and far-field tsunami observations are required for better tsunami detection and disaster preparedness with the help of improved travel time forecast. Within the context of mitigation study, knowledge of accurate time delay is thus important for tsunami early warning to minimize potential losses of buildings, properties, and lives. This can be possibly achieved by rapid analyses of tsunamigenic earthquakes and accurate prediction of arrival times hence time delays recorded at a network of regional stations.

Acknowledgements

The authors would like to thank anonymous reviewers for their best suggestions and invaluable comments upon this article from its simple form of an originally submitted version to a form of a high level quality required for publication in STH.

References

Allgeyer, S. and P. Cummins (2014), Numerical tsunami simulation including elastic loading and seawater density stratification, Geophys. Res. Lett., 41, 2368-2375, doi:10.1002/2014GL059348.

Cholifah, L. and T. Prastowo (2017), Travel time difference between estimated and observed values of the 2011 trans-oceanic Tohoku tsunami, Proc. 7th Basic Science International Conference (BaSIC), Malang: Faculty of Science, The University of Brawijaya.

Fine, I. V., E. A. Kulikov and J. Y. Cherniawsky (2013), Japan's 2011 tsunami: characteristics of wave propagation from observations and numerical modeling, Pure Appl. Geophys., doi:10.1007/s00024-012-0555-8.

Glimsdal, S., G. K. Pedersen, C. B. Harbitz and F. Løvholt (2013), Dispersion of tsunamis: does it really matter? Nat. Hazards Earth Syst. Sci., 13, 1507-1523, doi:10.5194/nhess-13-1507-2013.

Gusman, A. R., S. Murotani, K. Satake, M. Heidarzadeh, E. Gunawan, S. Watada and B. Schurr (2015), Fault slip distribution of the 2014 Iquique, Chile, earthquake estimated from ocean-wide tsunami waveforms and GPS data, Geophys. Res. Lett., 42, 1053-1060, doi:10.1002/2014GL062604.

Heidarzadeh, M., K. Satake, S. Murotani, A. R. Gusman and S. Watada (2014), Deep-water characteristics of the trans-Pacific tsunami from the 1 April 2014 Mw 8.2 Iquique, Chili earthquake, Pure Appl. Geophys., doi:10.1007/s00024-014-0983-8.

Inazu, D. and T. Saito (2013), Simulation of distant tsunami propagation with a radial loading deformation effect, Earth Planets Space, 65, 835-842, doi:10.5047/eps.2013.03.010.

Prastowo, T., L. Cholifah, L. O. Ngkoimani and L. O. Safiuddin (2017), Tsunami-magnetic signals and magnetic anomaly generated by tsunami wave propagation at open seas, Jurnal Pendidikan Fisika Indonesia, 13(1), 59-70.

Prastowo, T. and T. N. Ain (2015), Experiments on gravity current to examine concepts of hydrodynamics and mass conservation for incompressible fluids, Jurnal Pendidikan Fisika Indonesia, 11(1), 84-92.

Rabinovich, A. B., R. N. Candella and R. E. Thomson (2011), Energy decay of the 2004 Sumatra tsunami in the world ocean, Pure Appl. Geophys., 168, 1919-1950, doi:10.1007/s00024-011-0279-1.

Rabinovich, A. B., R. N. Candella and R. E. Thomson (2013), The open ocean energy decay of three recent trans-Pacific tsunamic, Geophys. Res. Lett., 40, 3157-3162, doi:10.1002/grl.50625.

Satake, K., Y. Nishimura, P. S. Putra, A. R. Gusman, H. Sunendar, Y. Fuji, Y. Tanioka, H. Latief and E. Yulianto (2013), Tsunami source of the 2010 Mentawai, Indonesia earthquake inferred from tsunami field survey and waveform modeling, Pure Appl. Geophys., 170, 1567-1582, doi:10.1007/s00024-012-0536-y.

Suppasri, A., K. Goto, A. Muhari, P. Ranasinghe, M. Riyaz, M. Affan, E. Mas, M. Yasuda and F. Imamura (2015), A decade after the 2004 Indian Ocean tsunami: the progress in disaster preparedness and future challenges in Indonesia, Sri Lanka, Thailand, the Maldives, Pure Appl. Geophys., 172, 3313-3341, doi:10.1007/s00024-015-1134-6.

Tsai, V. C., J. P. Ampuero, H. Kanamori and D. J. Stevenson (2013), Estimating the effect of earth elasticity and variable water density on tsunami speeds, Geophys. Res. Lett., 40, 492-496, doi: 10.1002/grl.50147.

Wang, D. (2015), An ocean depth-correction method for reducing model errors in tsunami travel time: application to the 2010 Chile and 2011 Tohoku tsunamis, Sci. Tsunami Hazards, 34(1), 1-22.

Watada, S. (2013), Tsunami speed variations in density-stratified compressible global oceans, Geophys. Res. Lett., 40, 4001-4006, doi:10.1002/grl.50785.

Watada, S., S. Kusumoto and K. Satake (2014), Traveltime delay and initial phase reversal of distant tsunamis coupled with the self-gravitating elastic earth, J. Geophys. Res., 119, 4287-4310, doi: 10.1002/2013JB010841.

Wessel, P. (2009), Analysis of observed and predicted tsunami travel times for the Pacific and Indian oceans, Pure Appl. Geophys., 166, 301-324, doi:10.1007/s00024-008-0437-2.